ONLINE SUPPORTING MATERIAL

SUPPLEMENTAL FIGURE LEGENDS

Supplemental Figure 1. Structure and purity of netrin proteins. (A) Amino acid comparison of netrins-1, -2, and -4. Netrins-1 and -2 are more closely related (overall 52% amino acid identity) than are netrins-1 and -4 (overall 31% amino acid identity). All three netrins are secreted, diffusible proteins. **(B)** Silver stain analysis of netrin protein preparations. To assess purity of the recombinant netrins used in our *in vitro* assays, 1 µg of mouse netrin-G1a, mouse netrin-1, chicken netrin-2, and mouse netrin-4 were analyzed by sodium dodecyl sulfate polyacrylamide gel electrophoresis followed by silver staining. Molecular weight standards were electrophoresed in the well on the left. A single band of molecular weight 65-70 kDa for netrin-G1a and of 75-80 kDa for netrins-1, -2, and -4 was observed with no other significant contaminating proteins. **(C)** Immunodepletion of protein preparations using antibodies against netrin-1 or netrin-4 removes the promigratory activity. Polyclonal goat antibodies (20 µg/ml) against mouse netrin-1 (αN1 IgG) and netrin-4 (αN4 IgG) or non-specific goat anti-mouse IgG antibodies (NS IgG; 20 µg/ml) bound to Protein G+ agarose beads were incubated with purified, recombinant netrin-1 and netrin-4 preparations (50 ng/ml) for 2 hours at 4^{o} C. Following removal of the beads, the protein preparations were loaded into Boyden chambers for migration assays using human microvessel endothelial cells (HMVEC). Immunodepletion using antibodies against netrin-1 and netrin-4 removed essentially all of the promigratory activity previously contained in these protein preparations. Non-immunodepleted netrin-1 and netrin-4 (50 ng/ml) stimulated approximately threefold

increased migration, as did an equimolar amount of vascular endothelial growth factor (VEGF; 13 ng/ml), compared to 0.1% BSA control (Ctl).

Supplemental Figure 2. Netrins promote endothelial cell migration, proliferation, and tube formation but not adhesion. (A) Netrin-1 (N1) and netrin-4 (N4) stimulate migration human microvessel endothelial cells (HMVEC), human umbilical vein endothelial cells (HUVEC), human umbilical artery endothelial cells (HUAEC), and human coronary artery endothelial cells (HCAEC). We obtained similar results for MS1 murine endothelial cells and for murine lung endothelial cells (data not shown). Migration towards 50 ng/ml netrin-1 and netrin-4, as well as towards an equimolar amount of VEGF (13 ng/ml), was compared to 0.1% BSA control (Ctl). **(B)** Proliferation of HMVEC after 72 hours in the presence of 10-200 ng/ml netrins-1 and -4 or 13 ng/ml VEGF. Equimolar amounts of the netrins and VEGF (50 ng/ml netrin or 13 ng/ml VEGF) produced similar increases in proliferation. Data points represent the mean ± SEM of 24 separate determinations (8 individual wells from each of three separate experiments). **(C)** Proliferation of HUVEC after 72 hours in the presence of 10-200 ng/ml netrins-1 and -4 or 13 ng/ml VEGF. **(D)** Netrin-1 and -4 (200 ng/ml) as well as VEGF (13 ng/ml) stimulate tube formation in HUVEC as compared to control treatment (0.1% BSA). Quantification of line length in formed tubes demonstrates that the stimulatory effect of netrins-1 and -4 on tube formation is similar in magnitude to that of VEGF. Data points represent the mean value ± SEM. **(E)** Endothelial cells do not adhere to netrins. Quantification of HUVEC adhesion to 96-well plates treated overnight at 4^{o} C with 0.1% BSA (control) or 10 µg/ml netrin-1, netrin-2, netrin-4, or fibronectin.

Each data point represents the mean ± SEM of combined data from two separate experiments where cells in 6 low power (10X) fields from duplicate wells were manually counted. **(F)** HUVEC adhesion to 96-well plates treated overnight at 4^{o} C with 0.1% BSA (control) or 10 µg/ml netrin-1, netrin-2, netrin-4, or fibronectin. Each panel represents a 10X light microscope field, and the scale bar in the left panel represents 100 µm.

Supplemental Figure 3. Netrin-induced endothelial cell migration does not require activation of the adenosine A2b receptor. (A) COS-7 cells overexpressing the Unc5b receptor or A2b were incubated with 2 nM netrin-1-alkaline phosphatase (netrin-1AP) or netrin-4-alkaline phosphatase (netrin-4AP) fusion proteins. The cells on the left side of each panel were first pretreated with a 10X molar excess of unlabelled netrins to demonstrate specificity of interaction. The cells were then washed and exposed to precipitating substrate. Representative light microscopy fields are shown. Control transfections with empty vector (pcDNA3.1) demonstrated no baseline interaction of netrins with COS-7 cells, whereas netrin-1AP binds to Unc5b-overexpressing COS-7 cells, and pretreatment with unlabeled netrin-1 blocks this interaction. Similar binding of Netrin-4AP to Unc5b-expressing cells was not observed. Neither netrin-1AP nor netrin-4AP binds to A2b overexpressing cells. Scale bar, 50 µm. **(B)** Human microvessel endothelial cells (HMVEC) were incubated in basal media containing 1.2% DMSO (control, netrin alone, and vascular endothelial growth factor) or in basal media containing 1 µM DPSPX (1,3-dipropyl-8-sulfophenylxanthine) or 600 µM enprofylline (3-propylxanthine) and 1.2% DMSO. DPSPX and enprofylline are antagonists of the

adenosine A2b receptor. DPSPX and enprofylline at concentrations well in excess of their K_i values have no significant effect on HMVEC migration induced by netrin-1 and netrin-4, a result similar to that of Stein et al for axon outgrowth.

Supplemental Figure 4. Trunk morphology is preserved in *netrin1a* morphants. Antibody staining shows that slow muscle cells (F59) and engrailed-positive cells (4D9), which include both muscle pioneers and a subset of fast muscle cells, are not disrupted in *netrin1a* morphants (**A**, **C** respectively) when compared to uninjected controls (**B**, **D** respectively). Confocal z-projections of 32hpf *fli*:*egfp* embryos; anti-GFP staining in *green*. 4D9 and F59 in *magenta*. **(E)** *Netrin1a* splice-blocking morpholino greatly reduces normal mRNA. Positions of *netrin1a* splice-blocking MO and RT-PCR primers relative to the exon/intron genomic structure of *netrin1a* (not to scale). **(F)** Total RNA was isolated from uninjected embryos and *netrin1a* morphants (5.6 ng MO), DNase-treated, and RT-PCR performed using primer pairs that amplify unspliced *netrin1a* pre-mRNA (*F1*+*R1*); properly spliced *netrin1a* mRNA (*F1*+*R2*); and *beta-actin* mRNA as a loading control (*beta-actin*). Normal mRNA seems to be completely abolished by injection of the *netrin1a* MO, while unspliced pre-mRNA levels are slightly increased. Reactions lacking reverse transcriptase (-RT) confirm that amplified bands reflect RNA and not genomic DNA.

Supplemental Figure 5. Local delivery of vascular endothelial growth factor (VEGF), netrin-1, or netrin-4 expression constructs promotes revascularization, reduces scar formation, and increases the number of vessels with smooth

muscle α-actin in mice with surgically-induced hindlimb ischemia. (A) Ratio of blood flow in the ischemic compared to the normal limb as assessed by laser Doppler perfusion imaging. Hindlimb ischemia was surgically induced in FVB/NJ mice by ligation and excision of the proximal femoral artery as described previously (*1*). VEGF, netrin-1, netrin-4 and empty vector DNA expression plasmids (50 µg DNA in 100 µl saline in each group) were locally injected into the right gastrocnemius muscle immediately, 7, 14 and 21 days after surgery. Laser Doppler perfusion imaging was used to record serial blood flow measurements over the course of 4 weeks postoperatively, as previously described (*2*). Ischemic hindlimbs injected with VEGF, netrin-1, or netrin-4 expression constructs demonstrated improved perfusion compared to those injected with empty vector (EV) beginning at day 7 following surgical induction of ischemia and plasmid injection. This improvement continued through day 28. **(B)** FITC-isolectin B4 staining of sections of gastrocnemius muscle 28 days after surgical induction of ischemia and initiation of plasmid injection is shown in the left panel. On the right is seen quantification of capillary density per high power field as determined by isolectin B4 staining in ischemic muscle 28 days after induction of ischemia. **(C)** The left panel demonstrates Masson's Trichrome staining of muscle cross section from animals on day 28 after surgical induction of ischemia and local injection of empty vector, VEGF, netrin-1, or netrin-4 DNA expression constructs. Areas of scar stain blue. Scar quantification is shown on the right, calculated as percentage area of the muscle bundle. Animals injected with VEGF, netrin-1, or netrin-4, had significantly less scar compared to animals injected with empty vector. **(D)** Staining of muscle cross sections with FITC-smooth muscle α-actin on day 28 after surgical induction of ischemia is seen

on the left. VEGF, netrin-1, netrin-4 and empty vector DNA expression plasmids (50 µg DNA in 100 µl saline in each group) were locally injected into the right gastrocnemius muscle immediately, 7, 14 and 21 days after surgery. On the right is displayed the quantification of vessels positive for staining with smooth muscle α-actin. Animals injected with netrin-1 plasmid had a greater density of smooth muscle α-actin-positive vessels.

Supplemental Figure 6. Local delivery of vascular endothelial growth factor (VEGF), netrin-1, or netrin-4 expression constructs into *db/db* animals increases capillary density of the sciatic vasa nervorum. (A) BS1 lectin (endothelial) staining of longitudinal and cross sections of sciatic nerves and BrdU staining of adjacent cross sections of sciatic nerves from *db/db* mice at 28 days following initiation of injection of empty vector, netrin-1, netrin-4, or VEGF. White arrowheads indicate representative structures that stained with both B1 lectin and BrdU, indicating endothelial structures with active cell division. Blue arrowheads indicate representative structures that stained with BrdU and not BS1 lectin. S100 staining of adjacent sections suggest that these structures are Schwann cells. Scale bar, 200 µm (longitudinal sections), 100 µm (cross sections). **(B)** Quantification of capillary density in the vasa nervorum of the sciatic nerves of *db/db* mice as assessed by BS1 lectin staining demonstrates increased capillary density in animals injected with the netrin-1, netrin-4, or VEGF constructs as compared to those injected with empty vector. (**C)** The number of cells per sciatic nerve cross section that stain for both BS1 lectin and BrdU is significantly greater ($P<0.05$) in *db/db* animals injected with netrin-1, netrin-4, or VEGF compared to animals injected

with empty vector. (**D**) The number of cells per sciatic nerve cross section that stain for both BrdU and S100 (Schwann cell) is significantly greater in *db/db* animals injected with netrin-1 than in animals injected with VEGF, netrin-4, or empty vector.

Supplemental Figure 7. Generation of Unc5b mutant mice. (**A**) Targeting strategy. Homologous recombination generates the *Unc5b*^{Neo} allele. FRT sites flank the neomycin cassette. Cre (Hprt-Cre) recombinase deletes exons 4-13, the region between lox P sites, resulting in the *Unc5b* deleted allele (*Unc5b*-). The transmembrane domain encoded by exon 9 is marked by a black bar. (**B and C**) Southern blot and PCR analysis of offspring from chimeras confirm germline transmission. The Southern probe and detected DNA fragments are indicated in (**A**). The PCR fragments amplified from wild-type and targeted alleles are approximately 100 bp and 150 bp, respectively. **(D)** PCR genotyping of offspring from *Unc5b* +/- and *Unc5b* +/- mating. For the *Unc5b* deleted allele (*Unc5b* -), an approximately 300 bp PCR fragment is amplified by the D2F and 2R primer set. For the *Unc5b* + allele, a 150 bp PCR product is amplified by the 2F and 2R primer set. **(E)** RT-PCR analysis confirms the lack of *Unc5b* transcripts in *Unc5b -/-* embryos but presence in *Unc5b* +/+ or +/- embryos. Actin was used as a loading control. No product is amplified without reverse-transcriptase (- RT).

Supplemental Figure 8. Vascular patterning of Unc5b +/+ and Unc5 -/- embryos are similar. **(A)** Vascular patterning of *Unc5b* +/+ and *Unc5 -/-* embryos are indistinguishable by PECAM staining at E10.5-E11.5. *Unc5b -/-* embryos do not show

any significant vascular patterning defects in the head, trunk region (side and dorsal views) and yolk sac compared to littermate controls. **(B)** Vascular patterning is not significantly altered before or after mice die at E12.0-E12.5. Unc5b mice were crossed to Robo4-AP mice to label vascular endothelial cells using alkaline phosphatase (AP) activity. At E12.0, *Unc5b -/-*;*Robo4-AP/+* mice are stained for AP activity and compared to the same staining of *Unc5b +/+*;*Robo4-AP/+* mice. Vasculature of yolk sac and tails of embryos in E12.0 are similar in *Unc5b +/+* and *Unc5b -/-* mice. Mice die in utero between E12.0 and E12.5. AP staining of yolk sac and tails from E12.5 *Unc5b -/-* ;*Robo4-AP/+* and *Unc5b +/+*;*Robo4-AP/+* embryos do not show significant vascular patterning differences, although *Unc5b -/-* embryos are necrotic. **(C)** IsolectinB4 staining at E10.5-E11.5. IsolectinB4 staining of hindbrain vessels at E10.5 and E11.5 shows similar patterning in mutant and wildtype mice. Scale bars, 0.2 mm.

Supplemental Figure 1

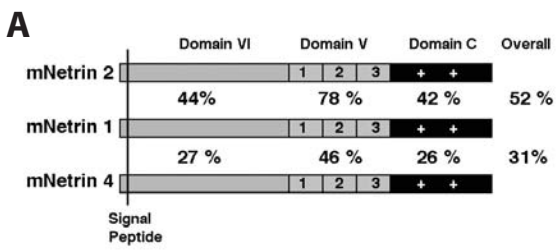

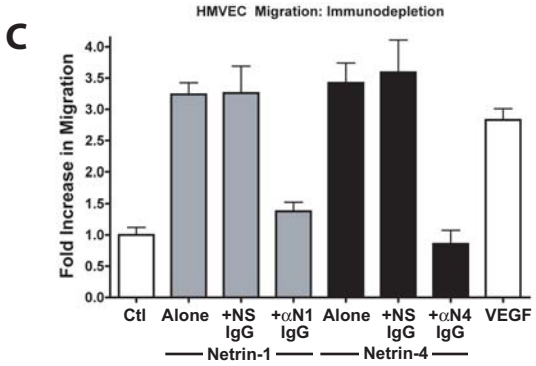

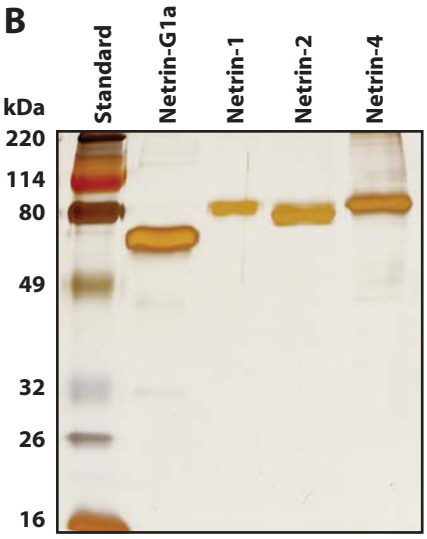

Supplemental Figure 2

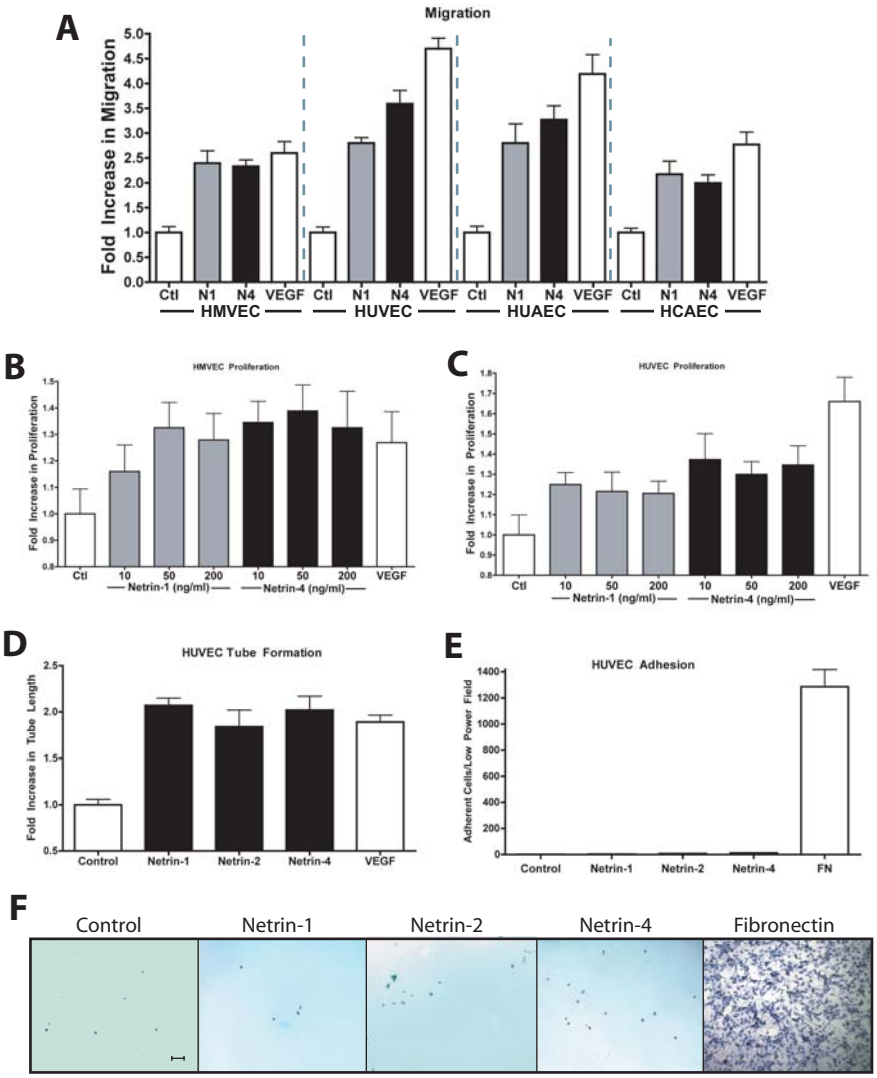

Supplemental Figure 3

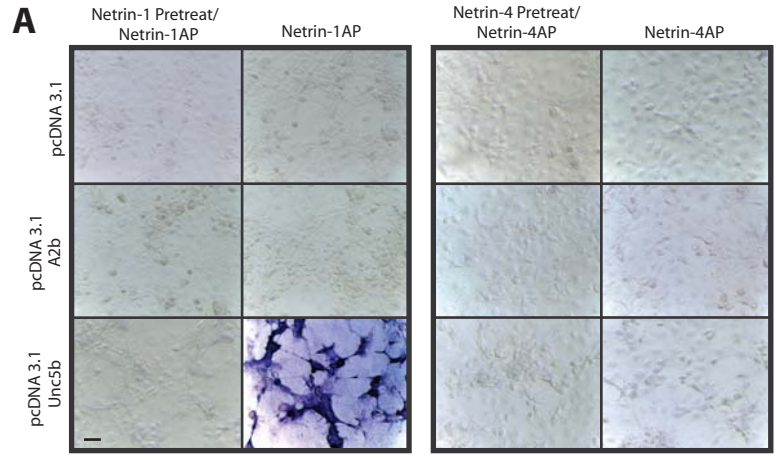

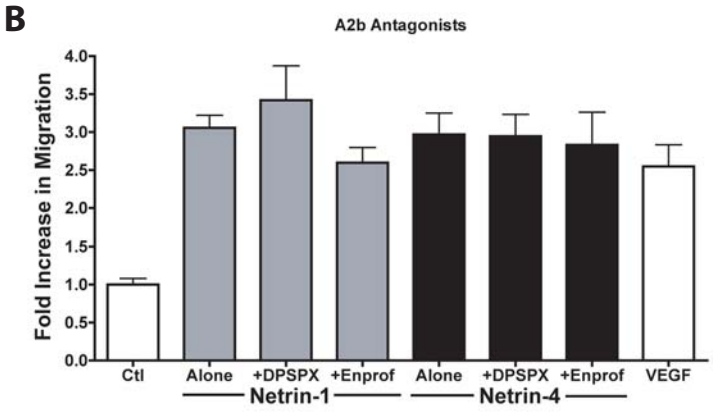

Supplemental Figure 4

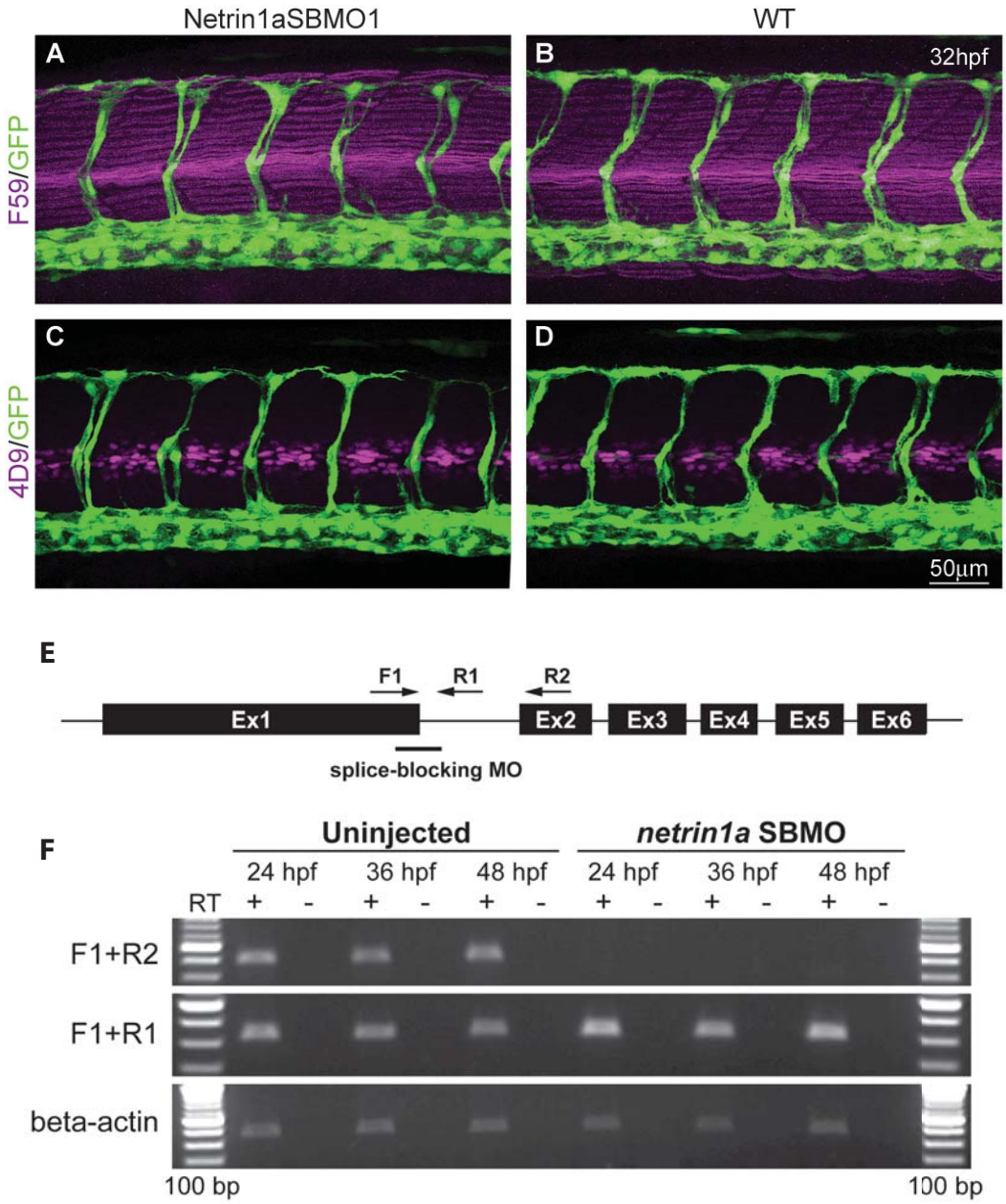

Supplemental Figure 5

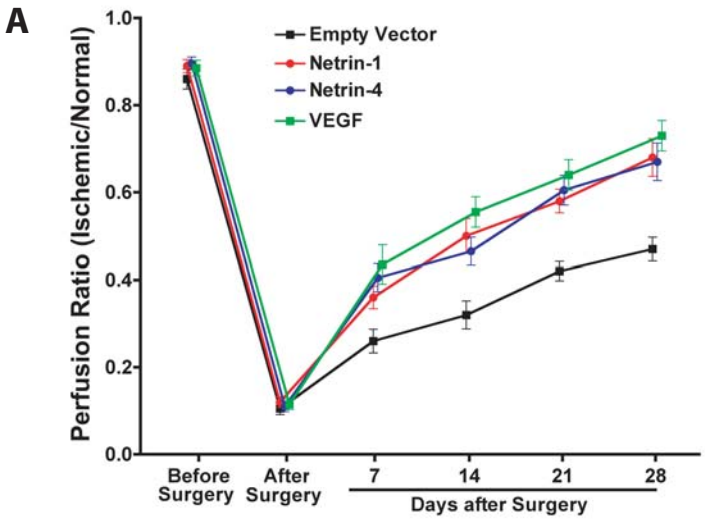

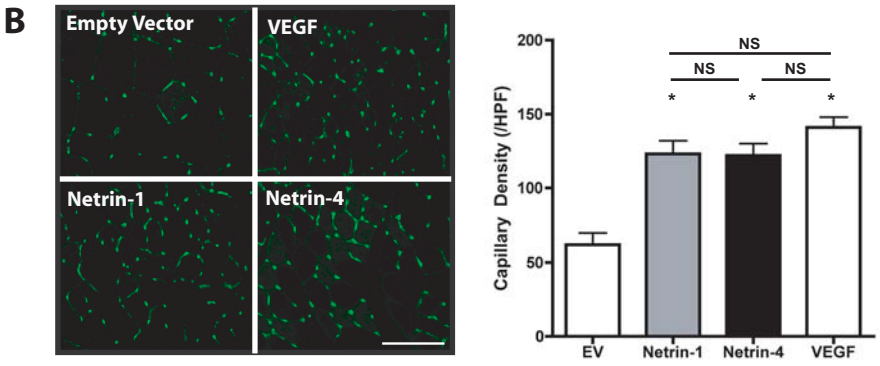

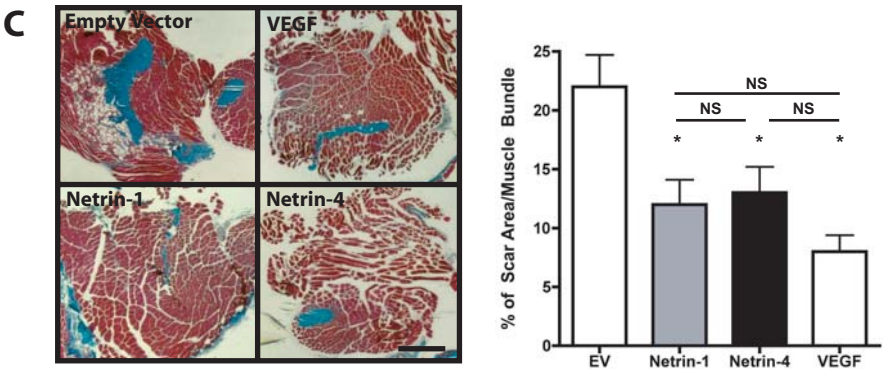

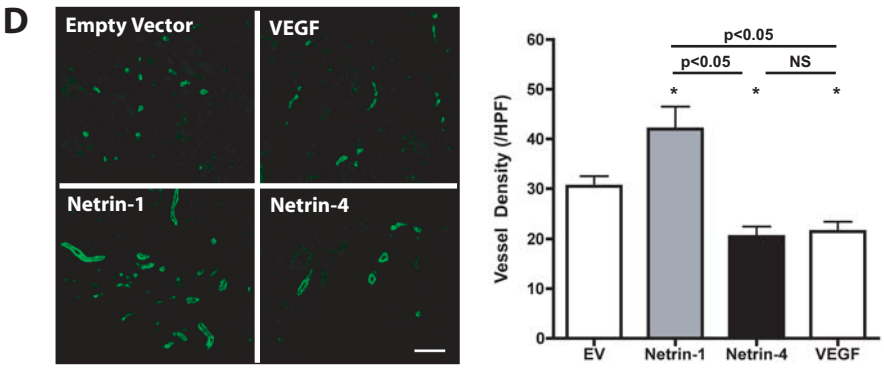

Supplemental Figure 6

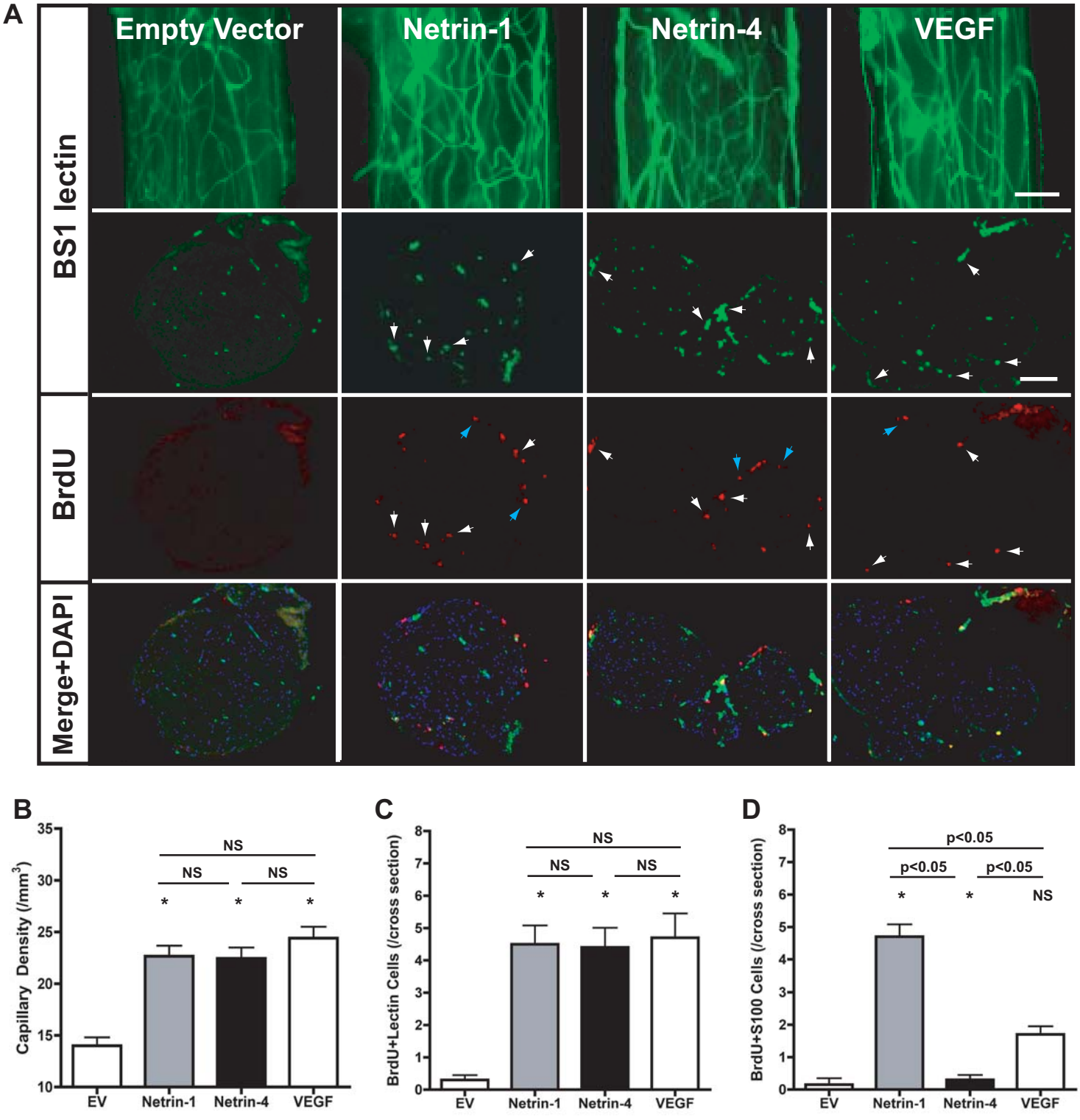

Supplemental Figure 7

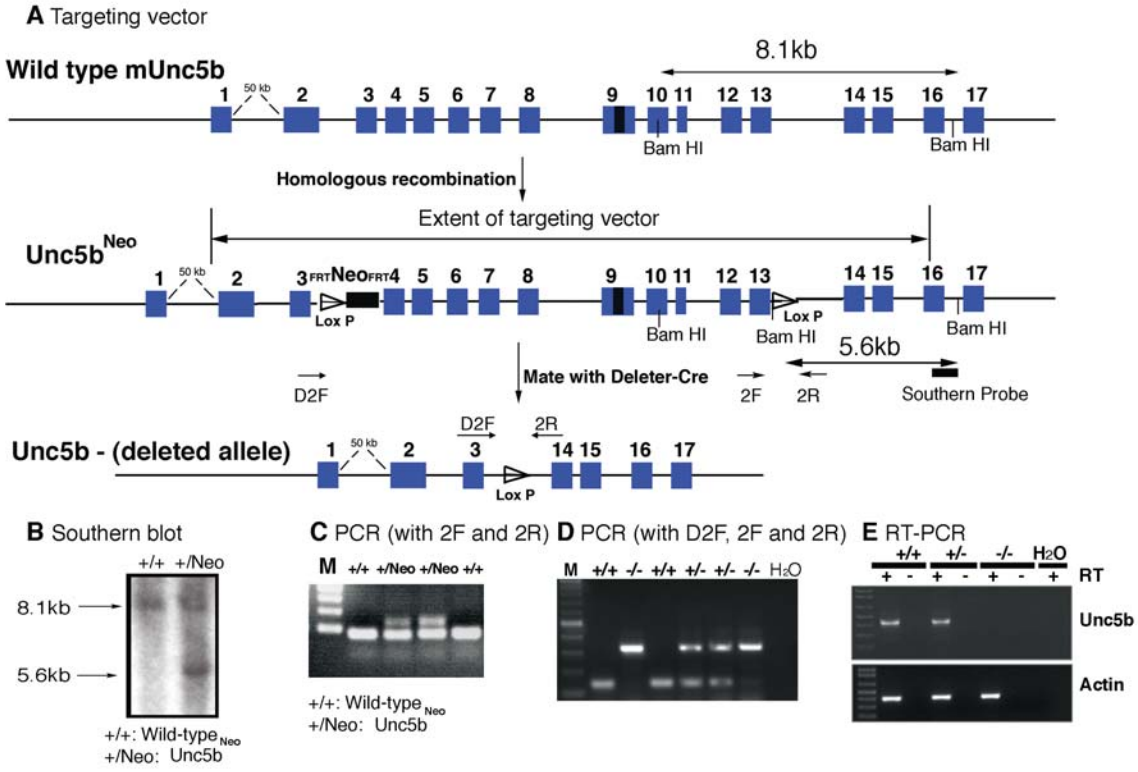

Supplemental Figure 8

A PECAM

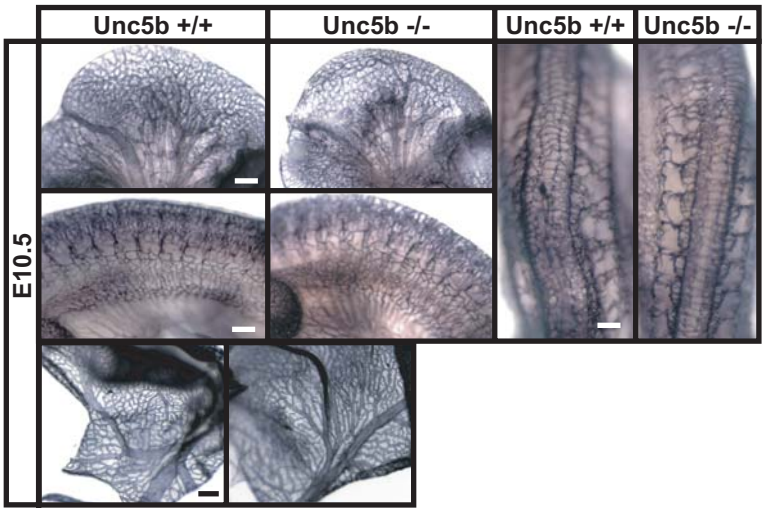

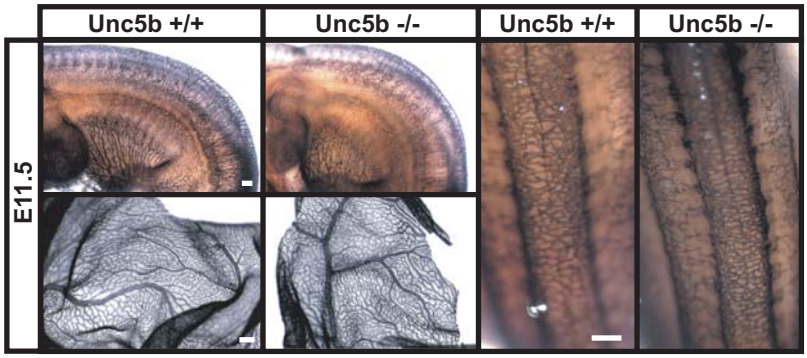

B Alkaline Phosphatase (Unc5b;Robo4-AP)

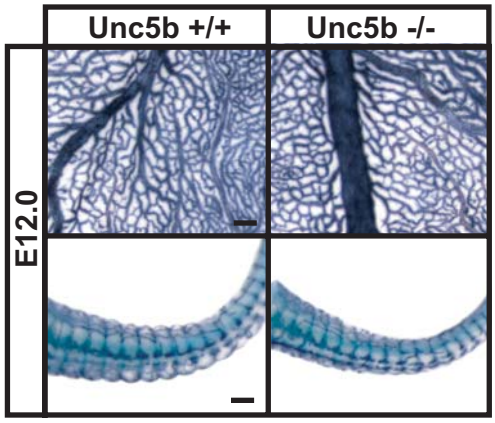

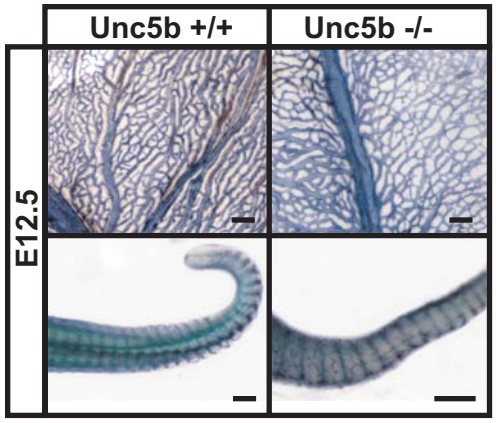

C Isolectin B4